Journal of Coordination Chemistry

Anion-induced assembly of 2-D Cd(II) complexes with $(4^2 \cdot 6)(4^2 \cdot 6^3 \cdot 8)$ topology based on ferrocenyl dicarboxylate and tripodal ligands

Xianju Shi [a] , Qingxia Li [a] , Yunshen Zhang [a] , Xiangling Chang [a] & Hongwei Hou [b]

[a] Puyang Key Laboratory of Functional Materials and Industrial Catalysis , Puyang Vocational and Technical College , Henan 457000, P.R. China

[b] Department of Chemistry , Zhengzhou University , Henan 450052, P.R. China
Published online: 08 Nov 2011.

PLEASE SCROLL DOWN FOR ARTICLE

Taylor & Francis
Taylor & Francis Group

Anion-induced assembly of 2-D Cd(II) complexes with $(4^2 \cdot 6)(4^2 \cdot 6^3 \cdot 8)$ topology based on ferrocenyl dicarboxylate and tripodal ligands

XIANJU SHI*†, QINGXIA LI†, YUNSHEN ZHANG†,
XIANGLING CHANG† and HONGWEI HOU‡

†Puyang Key Laboratory of Functional Materials and Industrial Catalysis, Puyang
Vocational and Technical College, Henan 457000, P.R. China
‡Department of Chemistry, Zhengzhou University, Henan 450052, P.R. China

Self-assembly of a flexible tripodal ligand, 1,3,5-tris(1,2,4-triazol-1-ylmethyl)benzene (ttmb) and organometallic carboxylate 1,1'-bis(3-carboxy-1-oxopropyl)-ferrocene (H_2bfcs) with $Cd(Ac)_2 \cdot 2H_2O$ or $CdCl_2 \cdot 2.5H_2O$ yields two 2-D binodal (3,4)-connected complexes $\{[Cd_2(bfcs)(Hbfcs)_2(ttmb)_2] \cdot 10H_2O\}_n$ (**1**) and $[CdCl(Hbfcs)(ttmb)]_n$ (**2**), exhibiting the same topological type $(4^2 \cdot 6)(4^2 \cdot 6^3 \cdot 8)$. Both exhibit a layer structure, which is generated through 1-D undulated ladders connected by organometallic carboxylate, $bfcs^{2-}$ (in **1**), or Cl^- (in **2**). Differential pulse voltammetry experiments indicate that half-wave potentials are slightly higher than that of H_2bfcs. Both complexes exhibit similar weak fluorescent emissions at room temperature.

Keywords: Ferrocenyl carboxylate; Tripodal ligand; Electrochemistry; Fluorescence

1. Introduction

Metal-organic frameworks (MOFs), a hybrid class of materials comprising inorganic nodes and organic struts, have been rapidly developed and received remarkable attention not only owing to fascinating structures but also potential applications such as functional materials in optics, electronics, and magnetism [1–6]. Among numerous synthetic approaches to construct MOFs, self-assembly using metal centers as nodes and organic spacers as linkers, has proven to be an effective way [7–10]. Organic ligands play important roles in obtaining structural diversity. Ligands that are flexible and possess versatile coordination modes are capable of satisfying many coordination preferences to facilitate formation of complexes with diverse frameworks and properties [11–15]. The selection of organic linker is, thus, a crucial step for this assembly reaction.

Ferrocenyl dicarboxylate ligands have rotatable ferrocene rings together with the double carboxylate groups and possess a variety of coordination modes [16, 17]. A flexible tripodal ligand, containing three functional groups and additional

---

coordination sites, can enrich the spatial connective modes of metal centers and extend the directionality of self-assembly [18–20]. The combination of these two types of ligands can provide more variability in response to diverse external conditions, which means that various complexes with rich structural diversity can be expected.

Herein, we present two 2-D binodal (3,4)-connected complexes induced by the addition of different Cd(II) salts to the two-ligand assembly system of ferrocenyl dicarboxylate (H_2bfcs) and a flexible tripodal ligand (ttmb). The structures are determined by single-crystal X-ray diffraction and the complexes are further characterized by elemental analysis, IR spectra, and powder X-ray diffraction (PXRD). The solution-state electrochemical and solid-state fluorescent properties were also investigated.

2. Experimental

2.1. *Materials and physical measurements*

H_2bfcs [21] and ttmb [22] were prepared according to the literature. Other starting reagents and solvents were purchased from commercial sources and used without purification. FT-IR spectra were recorded from KBr pellets from 400 to 4000 cm^{-1} on a Bruker Tensor 27 spectrophotometer. Elemental analyses (C, H, and N) were carried out on a FLASH EA 1112 elemental analyzer. PXRD patterns were recorded using Cu-Kα1 radiation on a PANalytical X'Pert PRO diffractometer.

2.2. *Synthesis of 1 and 2*

2.2.1. Synthesis of $\{[Cd_2(bfcs)(Hbfcs)_2(ttmb)_2] \cdot 10H_2O\}_n$ (1). An MeOH–H_2O (v/v 2 : 1) solution (6 mL) containing H_2bfcs (7.7 mg, 0.02 mmol) with pH = 7 controlled using CH_3ONa was added to methanol solution (2 mL) of Cd(Ac)$_2 \cdot$ 2H_2O (5.3 mg, 0.02 mmol), then a methanol solution (2 mL) of ttmb (6.4 mg, 0.02 mmol) was added dropwise to the above mixed solution, homogenized, and filtered. The resulting solution was allowed to stand in the dark at ambient temperature for 2 weeks. Crimson crystals were obtained in 39% yield (based on Cd). IR (cm^{-1}, KBr): 3116 m, 2916 m, 1667 s, 1561 s, 1423 m, 1257 m, 1134 m, 1086 m, 1019 m, 879 m, 751 m, 677 m, 478 m. Anal. Calcd for $C_{84}H_{100}Cd_2Fe_3N_{18}O_{28}$ (%): C, 45.81; H, 4.58; N, 11.45. Found: C, 45.37; H, 4.88; N, 11.04.

2.2.2. Synthesis of $[CdCl(Hbfcs)(ttmb)]_n$ (2). The synthesis procedure was similar to that of **1** except that CdCl$_2 \cdot$ 2.5H_2O (4.6 mg, 0.02 mmol) was used instead of Cd(Ac)$_2 \cdot$ 2H_2O. Yield: 42% (based on Cd). IR (cm^{-1}, KBr): 3123 m, 1668 s, 1557 m, 1513 s, 1453 s, 1233 m, 1132 s, 1020 m, 877 m, 751 m, 677 s, 511 m. Anal. Calcd for $C_{33}H_{32}CdClFeN_9O_6$ (%): C, 46.39; H, 3.78; N, 14.75. Found: C, 46.42; H, 3.96; N, 14.32.

Table 1.   Crystal data and structure refinement for **1** and **2**.

Complex	**1**	**2**
Empirical Formula	$C_{84}H_{100}Cd_2Fe_3N_{18}O_{28}$	$C_{33}H_{32}CdClFeN_9O_6$
Formula weight	2202.15	854.38
Temperature (K)	293(2)	293(2)
Wavelength (Å)	0.71073	0.71073
Crystal system	Triclinic	Triclinic
Space group	$P\bar{1}$	$P\bar{1}$
Unit cell dimensions (Å, °)		
a	12.779(3)	8.7719(18)
b	14.932(3)	12.919(3)
C	15.537(3)	15.028(3)
α	112.12(3)	78.06(3)
β	90.43(3)	82.91(3)
γ	104.93(3)	85.48(3)
Volume (Å^3), Z	2635.7(12), 1	1650.9(6), 2
Calculated density (g cm^{-3})	1.375	1.719
Absorption coefficient (mm^{-1})	0.877	1.226
$F(000)$	1108	864
Goodness-of-fit on F^2	1.098	1.065
$R_1[I > 2\sigma(I)]^a$	0.0935	0.0415
wR_2 (all data)^b	0.2587	0.0767
Largest difference peak and hole (e Å^{-3})	0.927 and −0.720	0.490 and −0.373

$^a R_1 = \sum ||F_o| - |F_c||/\sum |F_o|$.
$^b wR_2 = [\sum w(F_o^2 - F_c^2)^2/\sum w(F_o^2)^2]^{1/2}$.

2.3. *X-ray crystallographic analyses*

Single-crystal data of **1** and **2** were collected on a Rigaku Saturn 724 CCD diffractometer with graphite monochromated Mo-Kα radiation ($\lambda = 0.71073$ Å) at $20 \pm 1°$C and corrected for Lorenz-polarization effects. The structures were solved by direct methods and expanded using Fourier techniques. The non-hydrogen atoms were refined anisotropically and hydrogen atoms were placed at calculated positions. All calculations were performed using SHELXL-97 crystallographic software package [23] and refined by full-matrix least squares based on F^2 with isotropic thermal parameters. Crystallographic data and structure processing parameters for **1** and **2** are summarized in table 1. Selected bond lengths and angles of **1** and **2** are listed in table 2.

2.4. *Electrochemical properties determination*

Differential pulse voltammetries of **1** and **2** were performed by a CHI660B electrochemical analyzer utilizing the three-electrode configuration composed of a platinum working electrode, a platinum wire auxiliary electrode, and an Ag/AgCl reference electrode with pure N$_2$ gas inlet and outlet. The measurements were carried out in DMF solutions containing 0.1 mol dm^{-3} tetrabutylammonium perchlorate (n-Bu$_4$NClO$_4$) as supporting electrolyte, which had a 50 ms pulse width and a 16.7 ms sample width. The potential was scanned from 0.6 to 1.4 V at a scan rate of 20 mV s^{-1}.

Table 2. Selected bond lengths (Å) and angles (°) for **1** and **2**.

Complex **1**			
Cd(1)–O(4)	2.269(7)	Cd(1)–O(2)	2.307(6)
Cd(1)–N(1)	2.323(7)	Cd(1)–N(4)	2.324(6)
Cd(1)–N(7)	2.399(6)	Cd(1)–O(5)	2.598(9)
O(4)–Cd(1)–O(2)	87.2(3)	O(4)–Cd(1)–N(1)	134.0(3)
O(2)–Cd(1)–N(1)	137.9(2)	O(4)–Cd(1)–N(4)	93.2(2)
O(2)–Cd(1)–N(4)	88.7(2)	N(1)–Cd(1)–N(4)	96.0(2)
O(4)–Cd(1)–N(7)	99.6(3)	O(2)–Cd(1)–N(7)	87.7(2)
N(1)–Cd(1)–N(7)	78.2(2)	N(4)–Cd(1)–N(7)	166.6(2)
O(4)–Cd(1)–O(5)	51.9(3)	O(2)–Cd(1)–O(5)	139.1(3)
N(1)–Cd(1)–O(5)	82.5(3)	N(4)–Cd(1)–O(5)	93.4(3)
N(7)–Cd(1)–O(5)	97.7(3)		
Complex **2**			
Cd(1)–O(1)	2.329(3)	Cd(1)–N(6)	2.349(3)
Cd(1)–N(9)	2.412(3)	Cd(1)–N(1)	2.461(3)
Cd(1)–Cl(1)#1	2.5576(11)	Cd(1)–Cl(1)	2.8361(12)
Cl(1)–Cd(1)#1	2.5576(11)	O(1)–Cd(1)–N(6)	98.83(10)
O(1)–Cd(1)–N(9)	80.52(10)	N(6)–Cd(1)–N(9)	91.36(9)
O(1)–Cd(1)–N(1)	120.79(10)	N(6)–Cd(1)–N(1)	76.54(10)
N(9)–Cd(1)–N(1)	156.53(9)	O(1)–Cd(1)–Cl(1)#1	89.32(8)
N(6)–Cd(1)–Cl(1)#1	169.53(7)	N(9)–Cd(1)–Cl(1)#1	96.48(7)
N(1)–Cd(1)–Cl(1)#1	93.68(7)	O(1)–Cd(1)–Cl(1)	160.52(7)
N(6)–Cd(1)–Cl(1)	90.10(8)	N(9)–Cd(1)–Cl(1)	82.01(7)
N(1)–Cd(1)–Cl(1)	78.04(8)	Cl(1)#1–Cd(1)–Cl(1)	84.15(4)
Cd(1)#1–Cl(1)–Cd(1)	95.85(4)		

Symmetry transformations used to generate equivalent atoms in **2**: #1 $-x+2$, $-y+1$, $-z+1$.

2.5. *Fluorescent properties*

Fluorescent measurements for solid **1** and **2** were performed at room temperature using an HITACHI F-4500 Fluorescence Spectrophotometer. The excitation slit, as well as the emission slit, was 2 nm.

3. Results and discussion

3.1. *Description of crystal structures*

A single-crystal X-ray diffraction study reveals that **1** crystallizes in the triclinic space group *P*1. The local coordination environment around Cd(II) is shown in figure 1(a). Each six-coordinate Cd(II) is in a distorted octahedral geometry, formed by O2, O4, and O5 from two ferrocenyl carboxylate and N1 from a ttmb in the equatorial plane, and N4, N7 arising from two other ttmb ligands in axial positions. The Cd–O and Cd–N distances vary from 2.269(7) to 2.598(9) Å and 2.323(7) to 2.399(6) Å, respectively. In the tripodal ttmb, three triazole rings are connected through the benzene ring coupled with methylene moieties. Owing to the flexible methylene groups, ttmb can bend and rotate freely. On coordinating to Cd(II), one triazole ring lies outside the benzene plane, and the other two triazole rings lie in the reverse orientation outside the plane to form a capital "Y" (figure S1). The N6-containing triazole ring 1 is inclined to the benzene ring with an angle of 75.16°, and the corresponding values are
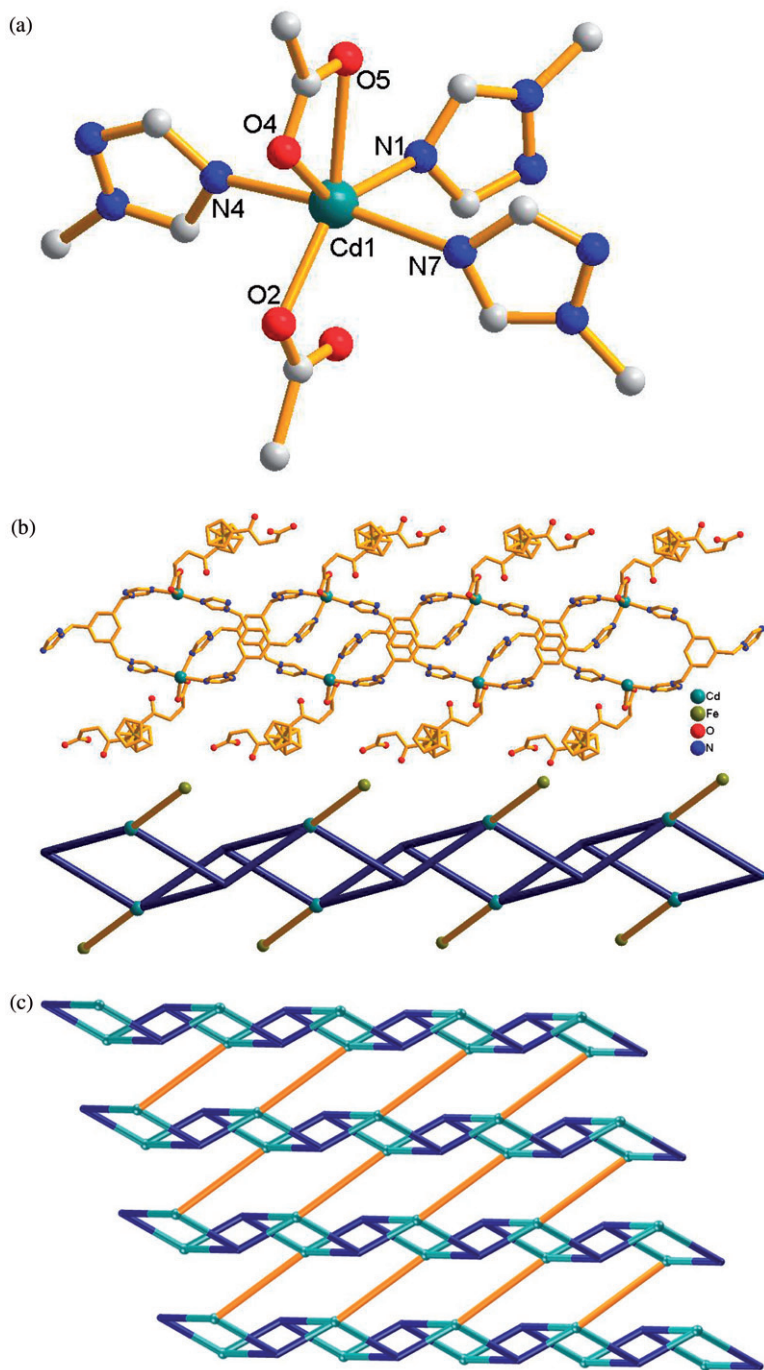
Figure 1. (a) Perspective drawing of **1** showing the local coordination environment around Cd(II). Hydrogen atoms and solvent molecules are omitted for clarity. (b) Schematic representation of the 1-D ladder-like structure of **1** involving terminal Hbfcs⁻. Hydrogen atoms and solvent molecules are omitted for clarity. (c) Topological representation of the 2-D structure of **1**.

84.22° and 89.64° for N2-containing ring 2 and N9-containing ring 3. The dihedral angles between rings 1 and 2, rings 1 and 3, rings 2 and 3 are 55.16°, 19.08° and 39.48°, respectively. In such *cis,trans,trans*-conformation, each ttmb, as a 3-connected ligand, coordinates to three different Cd(II) ions to form 1-D undulated ladder chains. Each Cd(II) is bonded by a terminal Hbfcs⁻, wherein one carboxylate adopts bidentate chelating coordination and the other remains protonated (figure 1b). In addition to terminal Hbfcs⁻, the completely deprotonated H_2bfcs ($bfcs^{2-}$) is present in the complex. The bis-monodentate organometallic carboxylate $bfcs^{2-}$ connects the 1-D undulated ladders to form a 2-D layer structure with Cd$\cdots$Cd distance of 12.27 Å. Topology analysis performed by OLEX [24] indicates that ttmb ligands are 3-connected nodes with Schäfli symbol $(4^2 \cdot 6)$ while the Cd(II) centers are 4-connected nodes with symbol $(4^2 \cdot 6^3 \cdot 8)$. Considering the stoichiometry, the whole net can be defined as a binodal (3,4)-connected $(4^2 \cdot 6)(4^2 \cdot 6^3 \cdot 8)$ topological type (figure 1c). The 2-D layers pack through extensive hydrogen-bonding that affords a 3-D supramolecular structure (figure S2).

Crystallographic analysis reveals that **2** crystallizes in the triclinic space group *P*1̄ with each Cd(II) center in a six-coordinate environment supplied by three nitrogen atoms from three ttmb, one oxygen atom from one Hbfcs⁻, and two chlorides (figure 2a). The bond distances of Cd–N range from 2.349(3) to 2.461(3) Å and Cd–O distance is 2.329(3) Å, which compares favorably to **1**. The combination of Cd(II) centers, terminal Hbfcs⁻, and *cis,trans,trans*-ttmb leads to a 1-D undulated ladder building block as in **1**. In contrast to **1**, the terminal Hbfcs⁻ of **2** is monodentate. The Cl⁻ functions as the linker to connect the ladders resulting in a 2-D layer structure (figure 2b). Topology analysis reveals that the framework of **2** is also classified as a binodal (3,4)-connected $(4^2 \cdot 6)(4^2 \cdot 6^3 \cdot 8)$ topological type based on two Cd(II) centers and two chlorides (figure 2c). The Cd$\cdots$Cd separation is 4.01 Å, shorter than **1**. Through the interlayer O–H$\cdots$O hydrogen-bonding between the non-deprotonated –OH groups of carboxylates and the non-coordinated oxygen atoms of monodentate carboxylates, the 2-D layers are packed together to form a 3-D supramolecular structure (figure S3).

3.2. *Electrochemical properties*

From reported studies [25, 26], high redox ability has been found to be one of the unique features of ferrocene and derivatives. The differential pulse voltammetries of **1** and **2**, as shown in figure 3, indicate that both exhibit a single peak within the potential range (from *ca* 0.6 to 1.4 V), corresponding to electron-transfer of ferrocene. The half-wave potentials ($E_{1/2}$) of **1** (0.956 V) and **2** (0.940 V) are slightly shifted to higher potential in comparison to that of H_2bfcs (0.908 V) [27]. The reason is that the electron-withdrawing nature of coordinated metal centers makes the ferrocene unit more difficult to oxidize [28], which has been demonstrated by previous transition metal–ferrocenyl systems [29, 30]. We also found that $E_{1/2}$ of H_2bfcs (0.908 V) shifted to higher value relative to free ferrocene (0.524 V), and the result could be attributed to electron-withdrawing ability of the carbonyl groups existing in H_2bfcs [31].

3.3. *Fluorescent properties*

The solid-state fluorescence spectra of **1**, **2**, free ttmb, and H_2bfcs were measured at room temperature. Phase purities of bulk samples of **1** and **2** were supported by PXRD
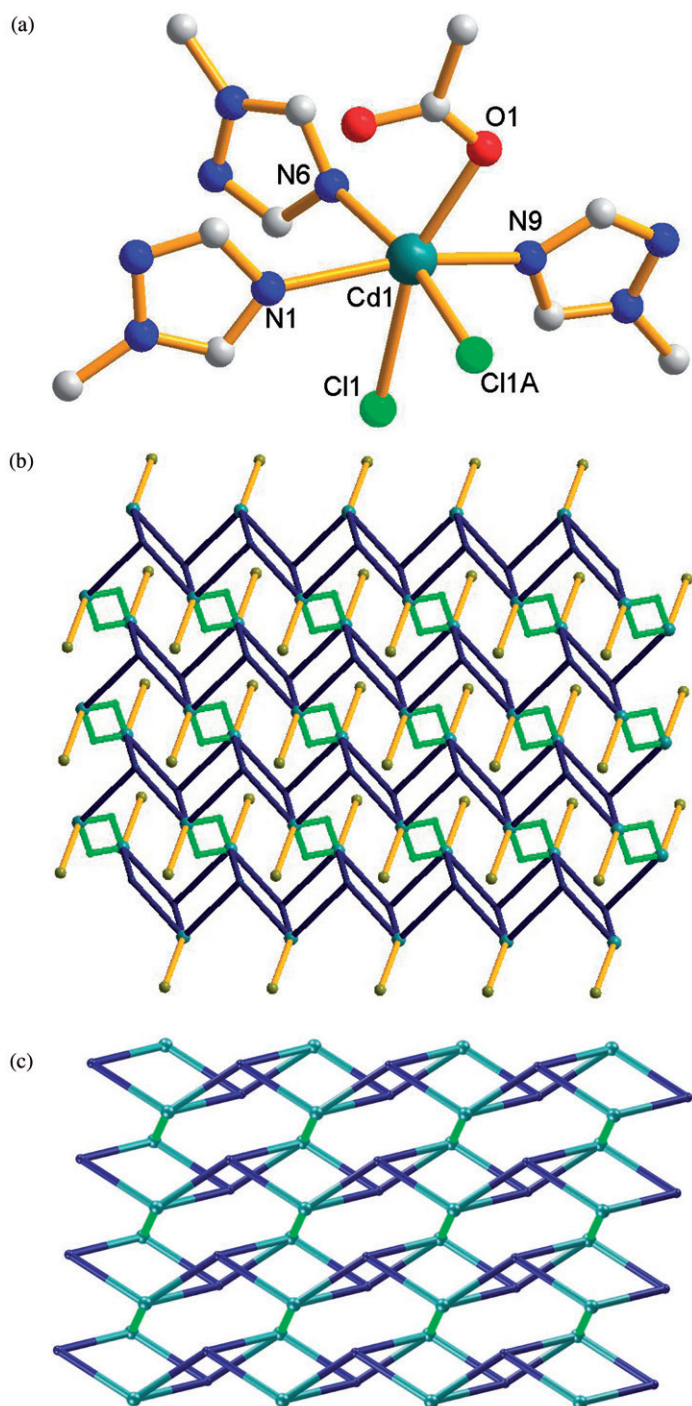
Figure 2. (a) Perspective drawing of **2** showing the local coordination environment around Cd(II). Hydrogen atoms are omitted for clarity. (b) Schematic representation of the 2-D network of **2** involving terminal Hbfcs⁻. (c) Topological representation of the 2-D structure of **2**.
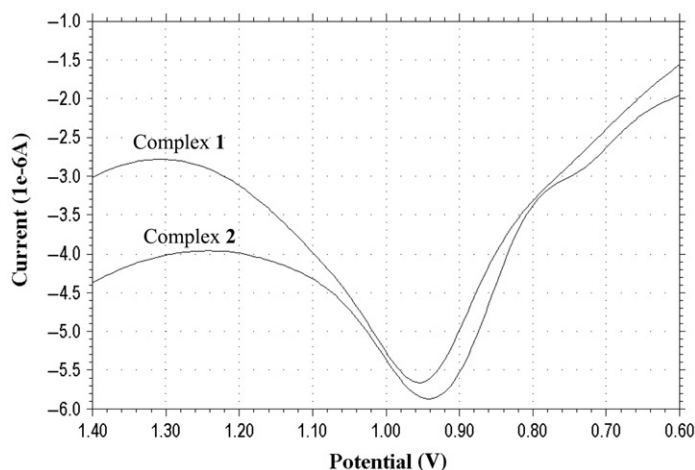
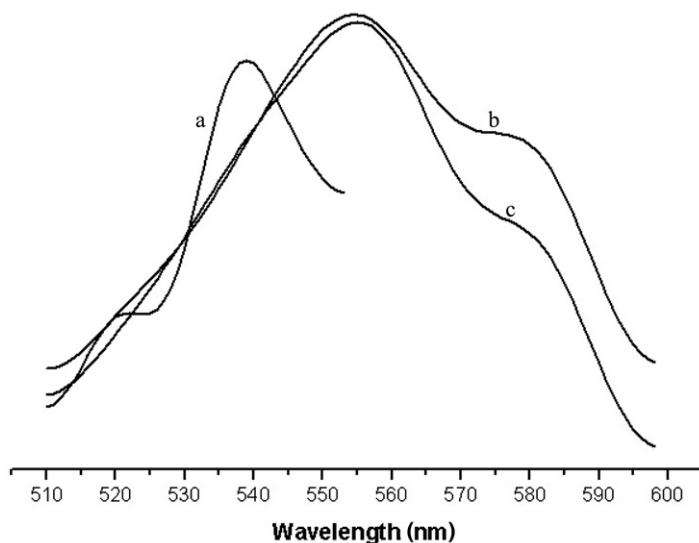Figure 3.   Differential pulse voltammogram of **1** (0.956 V) and **2** (0.940 V).

Figure 4.   Solid-state fluorescent emission spectra for: (a) H_2bfcs, (b) **1** and (c) **2**.

patterns, which match those simulated from the single-crystal X-ray diffraction data (figure S4, S5). Although ttmb is fluorescent with a strong emission band at 383 nm upon excitation at 336 nm, both complexes exhibit similar weak emissions with maximum intensity at about 556 nm ($\lambda_{ex} = 408$ nm) (figure 4). The emissions are tentatively assigned to intraligand fluorescent emission of the ferrocenyl dicarboxylate rather than metal-to-ligand charge transfer or ligand-to-metal charge transfer because a similar emission at 538 nm upon excitation at 395 nm is also observed for free H_2bfcs [32]. Moreover, fluorescence spectra of **1** and **2** exhibit slight red-shifts in

contrast to H$_2$bfcs, which is likely due to coordination of deprotonated H$_2$bfcs to Cd(II) resulting in a change in energy levels [33, 34]. Collectively, the results demonstrate that ferrocenyl dicarboxylate plays a dominant role in influencing the fluorescent properties of these two mixed-ligand complexes.

4. Conclusion

Using self-assembly of a flexible tripodal ligand and an organometallic dicarboxylate with different Cd(II) salts, we obtain two 2-D binodal (3,4)-connected complexes. Half-wave potentials were slightly higher than that of free H$_2$bfcs because of the electron-withdrawing nature of the coordinated metal centers. Both materials exhibit similar weak fluorescent emissions, assigned to intraligand fluorescent emission of the ferrocenyl dicarboxylate.

Supplementary material

CCDC 764392 and 764393 contain the supplementary crystallographic data for this article. These data can be obtained free of charge from The Cambridge Crystallographic Data Centre *via* www.ccdc.cam.ac.uk/data_request/cif

Acknowledgments

References

[1] T. Kaczorowski, I. Justyniak, T. Lipinska, J. Lipkowski, J. Lewinski. *J. Am. Chem. Soc.*, **131**, 5393 (2009).
[2] A.Y. Robin, K.M. Fromm. *Coord. Chem. Rev.*, **250**, 2127 (2006).
[3] Q.R. Fang, G.S. Zhu, Z. Jin, Y.Y. Ji, J.W. Ye, M. Xue, H. Yang, Y. Wang, S.L. Qiu. *Angew. Chem., Int. Ed.*, **46**, 6638 (2007).
[4] H. Li, M. Eddaoudi, M. O'Keeffe, O.M. Yaghi. *Nature*, **402**, 276 (1999).
[5] M. Tamura, M. Fujita. *Science*, **312**, 251 (2006).
[6] Y.T. Wang, G.M. Tang, Y.Q. Wei, T.X. Qin, T.D. Li, C. He, J.B. Ling, X.F. Long, S.W. Ng. *Cryst. Growth Des.*, **10**, 25 (2010).
[7] D.F. Sun, D.J. Collins, Y.X. Ke, J.L. Zuo, H.C. Zhou. *Chem. Eur. J.*, **12**, 3768 (2006).
[8] Y. Wang, X.Q. Zhao, W. Shi, P. Cheng, D.Z. Liao, S.P. Yan. *Cryst. Growth Des.*, **9**, 2137 (2009).
[9] Q.X. Yao, X.H. Jin, Z.F. Ju, H.X. Zhang, J. Zhang. *CrystEngComm*, **11**, 1502 (2009).
[10] L.Z. Chen, Y. Huang, R.G. Xiong, H.W. Hua. *J. Mol. Struct.*, **963**, 16 (2010).
[11] O.K. Farha, C.D. Malliakas, M.G. Kanatzidis, J.T. Hupp. *J. Am. Chem. Soc.*, **132**, 950 (2010).
[12] X.L. Wang, C. Qin, E.B. Wang, Z.M. Su. *Chem. Eur. J.*, **12**, 2680 (2006).

[13] Y.T. Wang, M.L. Tong, H.H. Fan, H.Z. Wang, X.M. Chen. *Dalton Trans.*, 424 (2005).
[14] Y.B. Dong, X. Zhao, R.Q. Huang, M.D. Smith, H. ZurLoye. *Inorg. Chem.*, **43**, 5603 (2004).
[15] R. Mondal, M.K. Bhunia, K. Dhara. *Cryst. Eng. Comm*, **10**, 1167 (2008).
[16] V. Lozan, A. Buchholz, W. Plass, B. Kersting. *Chem. Eur. J.*, **13**, 7305 (2007).
[17] J. Yang, J.F. Ma, Y.Y. Liu, S.L. Li, G.L. Zheng. *Eur. J. Inorg. Chem.*, 2174 (2005).
[18] H.K. Liu, H.Y. Tan, J.W. Cai, Z.Y. Zhou, A.S.C. Chan, S. Liao, W. Xiao, H.X. Zhang, X.L. Yu, B.S. Kang. *Chem. Commun.*, 1008 (2001).
[19] C. Tu, J. Lin, Y. Shao, Z.J. Guo. *Inorg. Chem.*, **42**, 5795 (2003).
[20] G.C. Xu, Y.J. Ding, T. Okamura, Y.Q. Huang, Z.S. Bai, Q. Hua, G.X. Liu, W.Y. Sun, N. Ueyama. *Cryst. Growth Des.*, **9**, 395 (2009).
[21] P.J. Graham, R.V. Lindsey, G.W. Parshall, M.L. Peterson, G.M. Whitman. *J. Am. Chem. Soc.*, **79**, 3416 (1957).
[22] H.K. Liu, W.Y. Sun, H.L. Zhu, K.B. Yu, W.X. Tang. *Inorg. Chim. Acta*, **295**, 129 (1999).
[23] G.M. Sheldrick. *SHELXL97: A Program for the Refinement of Crystal Structures from X-ray Data*, University of Göttingen, Göttingen, Germany (1997).
[24] O.V. Dolomanov, A.J. Blake, N.R. Champness, M. Schröder. *J. Appl. Cryst.*, **36**, 1283 (2003).
[25] L.K. Li, J.P. Li, H.W. Hou, Y.T. Fan, Y. Zhu. *Inorg. Chim. Acta*, **359**, 3139 (2006).
[26] D. Guo, Y.T. Li, C.Y. Duan, H. Mo, Q.J. Meng. *Inorg. Chem.*, **42**, 2519 (2003).
[27] X.J. Shi, H.W. Hou, L.W. Mi, Y.L. Sang, Y.T. Fan, R.Y. Liu. *Inorg. Chim. Acta*, **362**, 3364 (2009).
[28] E.M. Barranco, O. Crespo, M.C. Gimeno, P.G. Jones, A. Laguna, C. Sarroca. *J. Chem. Soc., Dalton Trans.*, 2523 (2001).
[29] A. Ion, M. Buda, J.C. Moutet, E. Saint-Aman, G. Royal, I. Gautier-Luneau, M. Bonin, R. Ziessel. *Eur. J. Inorg. Chem.*, 1357 (2002).
[30] Y.M. Xu, P. Saweczko, H.B. Kraatz. *J. Organomet. Chem.*, **637**, 335 (2001).
[31] M.W. Cooke, T.S. Cameron, K.N. Robertson, J.C. Swarts, M.A.S. Aquino. *Organometallics*, **21**, 5962 (2002).
[32] G.H. Wang, Z.G. Li, H.Q. Jia, N.H. Hu, J.W. Xu. *Cryst. Growth Des.*, **8**, 1932 (2008).
[33] V.T. Yilmaz, S. Hamamci, S. Gumus. *Chem. Phys. Lett.*, **425**, 361 (2006).
[34] Z.F. Tian, J.G. Lin, Y. Su, L.L. Wen, Y.M. Liu, H.Z. Zhu, Q.J. Meng. *Cryst. Growth Des.*, **7**, 1863 (2007).